

Finite element thermal study of the Linac4 plasma generator^{a)}

D. Faircloth,¹ M. Kronberger,^{2,b)} D. K uchler,² J. Lettry,² and R. Scrivens²

¹*STFC, Rutherford Appleton Laboratory, Chilton, Oxon OX11 0QX, United Kingdom*

²*BE-ABP, Hadron Sources & Linacs, CERN, CH-1211 Geneva, Switzerland*

(Presented 22 September 2009; received 17 September 2009; accepted 28 November 2009; published online 24 February 2010)

The temperature distribution and heat flow at equilibrium of the plasma generator of the rf-powered noncesiated Linac4 H⁻ ion source have been studied with a finite element model. It is shown that the equilibrium temperatures obtained in the Linac4 nominal operation mode (100 kW rf power, 2 Hz repetition rate, and 0.4 ms pulse duration) are within material specifications except for the magnet cage, where a redesign may be necessary. To assess the upgrade of the Linac4 source for operation in the high-power operation mode of the Superconducting Proton Linac (SPL), an extrapolation of the heat load toward 100 kW rf power, 50 Hz repetition rate, and 0.4 ms pulse duration has been performed. The results indicate that a significant improvement of the source cooling is required to allow for operation in the high-power mode of SPL. © 2010 American Institute of Physics. [doi:10.1063/1.3277144]

I. INTRODUCTION

The Superconducting Proton Linac¹ (SPL) project plays an important role in the proposed upgrade of the LHC injector chain. Using an extended version of the currently constructed Linac4 (Ref. 2) as front end, it should replace the presently employed proton linac (Linac2) and the Proton Synchrotron Booster (PSB). It is foreseen to operate the SPL in two modes. The low-power mode (LP-SPL) will inject a low-emittance H⁻ beam directly into an upgraded proton synchrotron (PS2) at 4 GeV, which will boost the LHC beam luminosity by one order of magnitude. In the high-power mode (HP-SPL), the beam energy will be increased further to 5 GeV and the duty factor from about 0.2% to several percent, which will open new possibilities for neutrino and radioactive ion beam production.³⁻⁶ On the other hand, this large increase in duty factor presents a major engineering challenge. A particular issue is the resulting high thermal load on the employed H⁻ source that will surpass that of the nominal operation mode of Linac4 by up to 75 times (Table I). In this paper, a study of the power dissipation in the Linac4 source is presented and the design changes required in a high power rf powered H⁻ source are detailed.

II. THE LINAC4 H⁻ SOURCE

The noncesiated Linac4 rf source⁷ is a copy of the H⁻ source that has been successfully developed and operated as part of the injector for the HERA accelerator at DESY.⁸ An outline of the plasma generator of the source is given in Fig. 1. Its main entities are the following: an ignition element used to ignite the plasma by a controlled electric discharge, a

plasma chamber made of Al₂O₃ ceramic, a copper antenna that feeds up to 100 kW, 2 MHz rf power into the plasma, a Delrin[®] magnet cage including an arrangement of 2 × 12 NdFeB cusp magnets and 10 NiZn ferrites, a drift region comprising a magnetic filter and a collar with a tiltable arrangement of extraction electrodes, and a ceramic disk that insulates the plasma generator electrically from the vacuum tank. The source is currently being commissioned and will be upgraded to the Linac4 nominal operation mode (I_{H-} = 80 mA, 0.25π mm mrad normalized emittance at 1 rms, 100 kW peak rf power) within the next few years.⁹

III. FINITE ELEMENT THERMAL STUDY OF THE LINAC4 SOURCE

In order to maintain the excellent performance of the Linac4 source also for SPL, the Linac4 source is used as the starting point for the development of a H⁻ source that can operate at the nominal operation mode of HP-SPL. To evaluate which components of the Linac4 source are critical for the heat transport, the temperature distribution and the heat flux inside the Linac4 plasma generator at thermal equilibrium are studied by finite element modeling using the ANSYS and ANSYS Workbench software packages. As the thermal load experienced in Linac4 operation already surpasses that in the original application of the source at DESY by a factor of 6 (Table I), this study serves also as a proof that the Linac4 H⁻ source can be operated at the thermal loads that are expected at Linac4.

The thermal study assumes that all rf power is coupled into the plasma. Ohmic losses in the antenna, the ferrites and the magnets, and rf power reflected back into the electronic circuit are not taken into account. After the power has been transferred, it is radiated toward the surfaces that confine the plasma volume. On the outside, the plasma generator is cooled by the emission of thermal radiation, convective air cooling, and the conduction to external heat sinks.

^{a)} Contributed paper, published as part of the Proceedings of the 13th International Conference on Ion Sources, Gatlinburg, Tennessee, September 2009.

^{b)} Electronic mail: matthias.kronberger@cern.ch.

TABLE I. H^- source nominal operational parameters of Linac4 and SPL. The operational parameters measured at DESY are shown for comparison.

	Linac4	LP-SPL	HP-SPL	DESY
I_{H^-} (mA)	80	80	80	40
ϵ_n^a (π mm mrad)	0.25	0.25	0.25	0.25
$q_{rf,peak}$ (kW)	100	100	100	30
Repetition rate (Hz)	2	2	50	3
Pulse length (ms)	0.4	1.2	0.4–1.2	0.15
Duty factor (%)	0.08	0.24	2–6	0.045
$q_{rf,avg}$ (W)	80	240	2–6k	13.5

^a ϵ_n : normalized emittance at 1 rms.

So far, the study has explored a steady state situation where the time structure of the heat load is neglected and only a constant average heat load $q_{rf,avg}$ is applied. This average heat load is first set to the average value of the Linac4 operation mode ($q_{rf,avg}=80$ W) and then increased to 2 kW to explore the thermal conditions within the plasma generator in the HP-SPL operation mode.

The model for plasma to wall radiation used in the thermal study is sketched in Fig. 2. The spatial distribution of the heat flux is modeled by approximating the plasma with an ellipsoidal black-body radiator centered at the position of the antenna coil. The temperature of the ellipsoid is set to a value for which the totally emitted power equals $q_{rf,avg}$. Table II provides an overview on the power dissipated in various regions of the plasma chamber. According to this model, the ceramic plasma chamber receives about 95% of the total heat load. This heat load is not uniformly distributed over the inner surfaces of the plasma chamber but shows a pronounced maximum at the position of the antenna coil (Fig. 2).

The thermal energy from plasma ignition is calculated from the ignition current and voltage and is found to be 0.18 J per pulse, corresponding to a time average thermal load of 0.36 W for Linac4 and 9 W for HP-SPL. This thermal load is distributed nonuniformly between cathode (60%) and anode (40%) to account for the larger fraction of the total kinetic energy carried by ions under the conditions of the gas discharge.

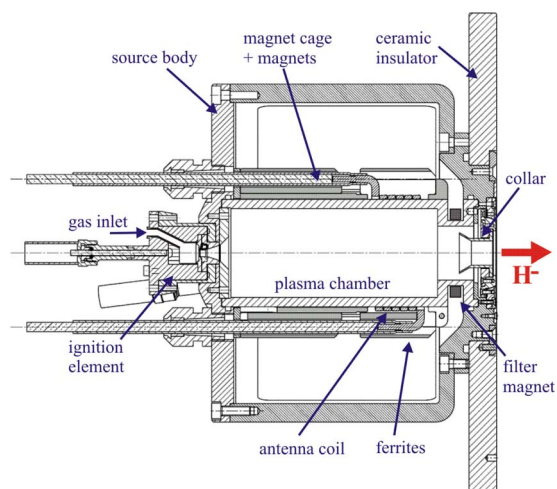


FIG. 1. (Color online) Outline of the Linac4 plasma generator.

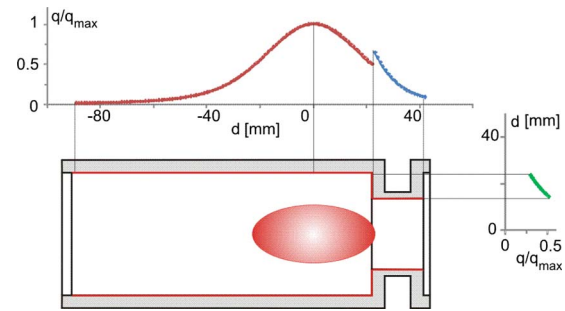


FIG. 2. (Color online) Simulated heat load distribution in the ceramic plasma chamber. d and q/q_{max} are the distance from the plasma ellipsoid center and the normalized heat flow, respectively. The curves on the top show the heat flow distribution along the cylindrical surfaces while the curve on the right shows the heat flow distribution of the end cap surface.

A realistic modeling of the heat flow inside the plasma generator is achieved by using thermal conductivities k and emissivities ϵ of the used materials from MatWeb (Ref. 10) and various other sources. The heat transfer through contacts is modeled by estimating thermal contact conductances with the model of Cooper *et al.*¹¹ and the gap conductance model given in Ref. 12. Convective air cooling of the outside surfaces is modeled by using a power law of the form¹²

$$q_C \propto (T_S - T_\infty)^{5/4} \cdot A_S, \quad (1)$$

where q_C is the power transported away by air convection from a surface with area A_S and temperature T_S . $T_\infty = 295$ K is the environmental temperature. This temperature is also used for the assumed external heat sinks of the source housing and the gas pipe.

IV. RESULTS AND DISCUSSION

The simulated temperature distribution in the plasma generator at the Linac4 peak power operation mode is illustrated in Fig. 3. The observed equilibrium temperatures T_{eq} range from T_∞ to a maximum of 410 K. Not surprisingly, the highest temperatures are found near the antenna coil where the thermal load reaches a maximum (Fig. 2). T_{eq} is within material specifications for all components except for the magnet cage, where temperatures above the maximum allowed operating temperature are reached close to the antenna. This implies that temperatures of the magnet cage should be monitored during Linac4 operation, and a redesign might be necessary if temperatures are found to reach critical values. The temperatures of the ferrites and the cusp magnets can reach up to 370 K, which causes a reduction of the

TABLE II. Dissipated power in different source components according to the simulated model. The numbers given for HP-SPL correspond to a time average rf power of 2 kW.

Component	q/q_{rf} (%)	Dissipated power (W)	
		Linac4	HP-SPL
Ignition element	1.0	1.2 ^a	30 ^a
Plasma chamber	95.3	76.2	1910
Collar	3.6	2.9	70

^aIncluding dissipated power from plasma ignition.

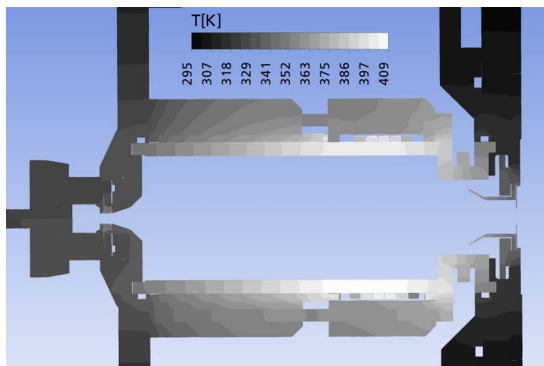


FIG. 3. (Color online) Simulated temperatures within the Linac4 plasma generator for $q_{rf,avg}=80$ W.

magnetic field strength of up to 8% for the cusp field and up to 30% for the ferrites relative to T_{∞} . Ohmic heating, which has not been considered in the study, may increase these temperatures even further. In fact, a preliminary electromagnetic study of the system indicates power losses of the order of several tens to a few hundred milliwatts per magnet, suggesting an additional temperature increase in the order of several kelvin.

The analysis of the heat flux allows for an identification of components and thermal contacts that are relevant for the heat transport in the Linac4 plasma generator. Due to the low thermal conductivity of the Delrin[®] magnet cage ($k=0.36$ W/mK¹⁰), the radial heat transport is suppressed in the vicinity of the plasma chamber. Instead, the heat flows mainly in axial direction into the source body from where it is removed by convective heat exchange with the surrounding air, by the emission of thermal radiation, or by flowing toward the heat sinks of the source housing and the gas pipe.

Although this cooling scheme appears to be sufficient for Linac4 operation, the suppression of the radial heat flow at the plasma chamber is expected to become increasingly problematic at higher power levels as the small cross section of the plasma chamber, the strongly decreasing thermal conductivity of the Al₂O₃ ceramic with temperature, and the small contact surfaces at the front and back end through which the thermal flow is guided into the source body limit the axial heat flow. Indeed, when the heat load from the plasma is pushed toward 2 kW, these limitations lead to a massive temperature increase, and overcritical temperatures are reached in almost every component of the plasma generator. A similar situation is present in the collar and the ignition element where the heat flow is limited by low thermal conductivity materials and nonideal thermal contacts.

The results indicate that major changes are necessary to design an ion source of the Linac4 type that is capable of operating at the HP-SPL nominal operation mode. These changes include the implementation of dedicated cooling circuits at positions where an efficient removal of heat is re-

quired, the replacement of materials used in the Linac4 source by materials with better heat conductivity, and the optimization of thermal contact conductances (for instance by brazing of conductors and insulators). Following this line, a plasma generator prototype that can withstand the high thermal loads experienced in the HP-SPL operation mode has been developed. The design of this device is discussed in detail in Ref. 13.

V. CONCLUSIONS AND OUTLOOK

A finite element thermal study of the Linac4 H⁻ plasma generator has been performed for the nominal operation modes of Linac4 (100 kW rf power, 0.08% duty cycle) and HP-SPL (100 kW rf power, 2% duty cycle). Within our assumptions, it is shown that in the nominal operation mode of Linac4, T_{eq} is within material specifications for all components except the magnet cage, for which critical temperatures are reached. The reduction of the radial heat flow due to the Delrin[®] magnet cage leads to a large increase in T_{eq} in the HP-SPL nominal operation mode and an operation of the Linac4 H⁻ source is excluded at these power levels. The design changes necessary to arrive at a high duty factor rf H⁻ ion source have been evaluated and have led to the development of a plasma generator prototype for SPL.

ACKNOWLEDGMENTS

The authors would like to thank M. Paoluzzi, E. ChauDET, and D. Steyaert for their help and assistance. This project has received funding from the European Community's Seventh Framework Programme (FP7/2007–2013) under the Grant Agreement No. 212114.

- ¹M. Baylac, F. Gerigk (ed.), E. Benedico-Mora, F. Caspers, S. Chel, J. M. Deconto, R. Duperrier *et al.*, CERN Report No. 2006–006, 2006.
- ²L. Arnaudon, P. Baudreghien, M. Baylac, G. Bellodi, Y. Body, J. Borburgh, P. Bourquin *et al.*, CERN-AB Report No. 2006–084 ABP/RF, 2006.
- ³P. Zucchelli, *Phys. Lett. B* **532**, 166 (2002).
- ⁴J. E. Campagne and A. Caze, CERN-NUFACT-NOTE 142, 2004, <http://cdsweb.cern.ch/record/806547>.
- ⁵The International Design Study of the Neutrino Factory, <https://www.ids-nf.org/wiki/FrontPage>.
- ⁶F. Gerigk and R. Garoby, Proceedings of the 39th ICFA Advanced Beam Dynamics Workshop on High Intensity High Brightness Hadron Beams, 2006 (unpublished), <http://cdsweb.cern.ch/record/961205>.
- ⁷D. Küchler, T. Meinschad, J. Peters, R. Scrivens, *Rev. Sci. Instrum.* **79**, 02A504 (2008).
- ⁸J. Peters, Proceedings of PAC05, Knoxville, TN, 2005 (unpublished), p. 788.
- ⁹M. Kronberger, D. Küchler, J. Lettry, Ø. Midttun, M. O'Neil, M. Paoluzzi, and R. Scrivens, *Rev. Sci. Instrum.* **81**, 02A708 (2010).
- ¹⁰MatWeb material database, <http://www.matweb.com>.
- ¹¹M. G. Cooper, B. B. Mikic, and M. M. Yovanovich, *Int. J. Heat Mass Transfer* **12**, 279 (1969).
- ¹²*Handbook of Heat Transfer*, 3rd ed., edited by W. M. Rohsenow, J. P. Hartnett, and Y. I. Cho (McGraw-Hill, New York, 1998).
- ¹³J. Lettry, M. Kronberger, R. Scrivens, E. ChauDET, D. Faircloth, G. Favre, J.-M. Geisser *et al.*, *Rev. Sci. Instrum.* **81**, 02A723 (2010).